INTERNATIONAL JOURNAL OF
ENERGY AND ENVIRONMENT

Volume 2, Issue 4, 2011 pp.701-716

Journal homepage: www.IJEE.IEEFoundation.org

Heat transfer characteristics of R410A during its evaporation inside horizontal tube

M. Fatouh, A.B. Helali, M.A.M. Hassan, A. Abdala

Mechanical Power Engineering Department, Faculty of Engineering at El-Mattaria, Helwan University, Cairo, Egypt.

Abstract
Evaporative local heat transfer coefficients of R22 and R410A are determined in electrically heated a smooth horizontal copper tube with inner diameter of 9.525 mm and length of 1000 mm. Experiments are carried out varying: the vapor quality (0.1:1), the heat fluxes (10:29) kW/m^2 and the evaporation temperatures (-5:5ºC) at mass flux of 100 kg/m^{2}s. Effect of the above operating parameters on heat transfer coefficients are investigated and reported in graphical forms. Experimental results showed that the heat transfer coefficients of R410A are better than those of R22, by about 17% and 14% during the lower and higher value of evaporating pressures and heat flux, respectively. The modified Kattan model results were found to be in much better agreement with the experimental results than the correlations from Gungor [12], Shah [20] and other correlations.

Keywords: Flow boiling; Horizontal; R22; R410A; Smooth tube.

1. Introduction

Several researches and development activities are proved that R22 has a bad effect on the environment such that ozone depletion and global warming and thus it will be phased out by the year 2030 according to Montreal Protocol [1]. Therefore, the research for a replacement of R22 has been intensified in recent years. The near azeotropic refrigerant mixture of R410A, a mixture of 50 wt.% R32 and 50 wt.% R125, has been considered as one of the primary replacements for R22 in the air-conditioning system applications [2]. Recently, air-conditioning systems with R410A have been developed and sold on market. However, there are limited heat transfer data of R410A for 9.525 mm inner diameter tube available. Kyu et al. [3]determined the evaporating flow patterns and heat transfers of R22 and R134a in small diameter tubes of 1.77, 3.36 and 5.35 mm. Greco [4] carried out an experimental study to investigate the characteristics of the evaporation heat transfer for different fluids (R22, R134a, R404A, R410A, R507, R407C and R417A) inside smooth horizontal stainless tube (6 mm ID, 6 m length). Shin et al. [5] determined experimentally convection boiling heat transfer of pure refrigerants and refrigerant mixtures in a horizontal stainless tube (7.7 mm, 5.9 m length). Zhang and Yuan [6] experimentally investigated heat transfer correlation for evaporation of refrigerant mixture R417A flowing inside smooth horizontal tube of 9.52 mm and two microfin tubes of 9.505 and 9.504 mm. Mcjimsey [7] experimentally investigated the effect of oil on convective heat transfer and pressure drop of R410A inside smooth tube (8 mm, 2.7 m). Park and Hrnjak [8] investigated R744 and R410A flow boiling heat

transfer, pressure drop, and flow pattern at low temperatures in a horizontal smooth tube (6.1 mm ID, 150 mm length).

The above review revealed that little available information on heat transfer characteristic of R410A inside tube diameter of 9.525 mm. Thus, the present work aimed to (1)determine the local heat transfer coefficients of R22 and R410A during convective boiling in a smooth horizontal copper tube with inner diameter 9.525 mm electrically heated; (2) Investigate deeply the influence of vapor quality, evaporation temperatures, heat flux and refrigerant fluid thermo-physical properties on the flow boiling characteristics; and (3) Investigate new heat transfer model which matches operating conditions in the industrial applications.

2. Test rig description and experimental procedures

A schematic diagram of the experimental apparatus is shown in Figure 1. which indicates the location of the sensors. The test facility consists of a refrigerant circuit and water path. In refrigerant circuit, the refrigerant passes firstly through electrical preheaters and then through test section, in which the refrigerant is heated by electric heater. The refrigerant exits the test section and goes through superheater, a rotary compressor, a water-cooled condenser, receiver, filter dryer and finally flashing through capillary tubes. The refrigerant circuit also includes gate valves, pressure controllers, piezoelectric transducer with range 0:8 bar and accuracy ±0.001 bar and K-type thermocouples. The water mass flow rate is controlled by a valve that restricts the flow of water. The water mass flow rate is also measured by digital balance and stopwatch.

The test section consists of a horizontal copper tube with inner diameter 9.525 mm, tube wall thickness is 5.19 mm and its length is 1000 mm as shown in Figure 2. The test section is instrumented with temperatures sensors and piezoelectric transducer. In the test section, K-type thermocouples are used for temperature measurement. Thermocouples are placed in three positions each position contains four thermocouples at top, bottom, and two sides and used to measure mean external surface temperature. All thermocouples are used after being revised with a standard thermometer. All thermocouples were carefully and accurately calibrated to an accuracy of ±0.1^{o}C compared to precision thermometer. The tube is electrically heated by Joule effect. A direct electrical current supplied by a feed current device circulates on the surface of the tube. The heat flux is changed by varying the direct electrical current. The heat flux supplied along the tube can be safely assumed to be constant, along the axis. The saturation temperature was calculated from the measured saturation pressure using the EES (Engineering Equation Solver) and verified with two thermocouples that measure the refrigerant temperature at the inlet and outlet of the test section

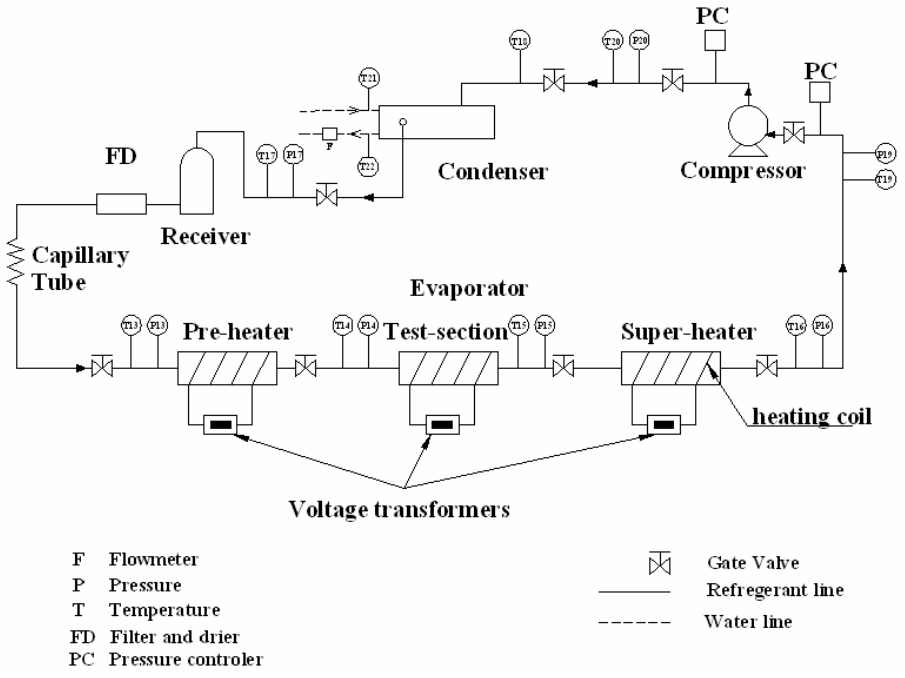

Figure 1. Schematic diagram of experimental apparatus

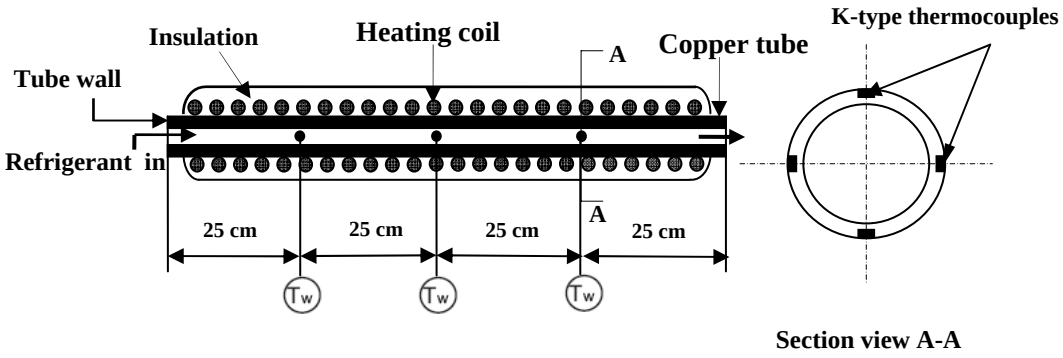

Figure 2. Details of test section for evaporating heat transfer

3. Data reduction

An analysis is needed to calculate the evaporating heat transfer coefficients from the experimental data. The data reduction process is described below. The heat transfer rate supplied from electric coil(Q_{coil}) to outside wall surface of copper tube in an evaporator is calculated using equation (1) as reported by [3], and the heat flux supplied from inside wall surface of copper tube ($q_{e,r}$)to refrigerant is calculated using equation (2)

$$Q_{coil} = \zeta \cdot V \cdot I \tag{1}$$

$$q_{e,r} = \frac{Q_{coil}}{\pi \cdot d \cdot L} \tag{2}$$

where, ζ is a heating coefficient which is defined as a ratio between output power and input power. It can be stated that both input and output powers are measured and ζ is calculated and reported in Table 1 which reveals that average value of ζ is about 0.92. V is the input voltage, I is the input electric current, L is the length of test section and d is the inner diameter of copper tube. The local heat transfer coefficient of refrigerant during evaporating process (α)[W/m^2 ·K] is calculated by the following equation,

$$\frac{1}{\alpha} = \frac{\left(T_{wo} - T_{sat}\right)}{q_{e,r}} - \frac{\ln\left(d_o / d_i\right) d_i}{2k} \tag{3}$$

where, T_{wo} is the average outside measured wall temperature, T_{sat} is the saturation refrigerant temperature and k is the thermal conductivity of copper [W/m K]. Average vapor quality is calculated by the following equation,

$$x_{avg.} = \frac{x_{in} + x_{out}}{2} \tag{4}$$

where, x_{in} is the inlet dryness fraction of refrigerant to the test section, which is calculated by the following equation

$$x_{in} = \frac{h_{in} - h_{L,in}}{h_{LG,in}} \tag{5}$$

h_{in} is the inlet specific enthalpy of the refrigerant at the outlet of preheater , which is determined by applying an energy balance on the preheater

$$h_{in} = h_1 + \frac{Q_{PH}}{\dot{m}_{ref}} \tag{6}$$

Table 1. Values of heating coefficient

$Power_{in}$	23.13	67.50	210	328.13	973.13	1150
$Power_{OUT}$	20.81	60.80	200	300	876	1069
ζ	0.90	0.90	0.93	0.91	0.90	0.93

x_{out} is the exit dryness fraction of refrigerant from test section can be determined from

$$x_{out} = \frac{h_{out} - h_{L,out}}{h_{LG,out}} \tag{7}$$

h_{out} is the exit enthalpy of the refrigerant is determined by applying an energy balance on the test section

$$h_{out} = h_{in} + \frac{Q_{TS}}{\dot{m}_{ref}} \tag{8}$$

Uncertainties in the experimental data were calculated using the analysis suggested by Holman (1978). The experimental uncertainties evaluated with the error analysis are of ±1.7%, as regards the heat flux, and of ±1.6% for the refrigerant mass flux. The error analysis for the heat transfer coefficient are ±4.055%.

4. Experimental results

In the present work, the experiments are performed for pure and mixed refrigerants (R22 and R410A) varying the evaporating temperature (-5:5°C), the heat flux (10:29 kW/m^2) and vapor quality (0.1: 1.0). The effect of the above parameters on flow pattern maps and the heat transfer coefficient is presented in graphical forms. Comparisons of the experimental results with the reported correlations in literature are discussed in details.

4.1 Flow pattern map

The latest version of the flow pattern map of Kattan et al. [21] is used for the evaluation of two phase flow regime. This map provides the transition boundaries (calculated from their underlying transitions equations, as described in Appendix (A)) on a linear-linear graph with mass velocity plotted versus vapor fraction for the particular fluid and flow channel. Figure 3. shows variation of mass flux with vapor quality at different operating conditions. It can be seen from Figure 3. that the flow pattern is slug and stratified wavy from the inlet section to a quality between 31% and 40%, depending on test conditions. Clearly, a stratified wavy is achieved, as higher vapor content.

4.2 Influence of operating parameters on heat transfer coefficients

In order to determine the characteristics and the mechanism of convective boiling, the influence of vapor quality, heat flux, evaporating pressure, refrigerant fluid thermo-physical properties on heat transfer coefficients is investigated.

4.2.1 Effect of vapor quality on evaporative heat transfer

Evaporative local heat transfer coefficients for R410A and R22 as a function of vapor quality are shown in Figure 4. It can be seen that the heat transfer coefficient increases with vapor quality. This can explained by the fact that as the flow proceeds downstream and vaporization takes place, the void fraction increases, thus decreasing the density of the liquid–vapor mixture. As a result, the flow

accelerates enhancing convective transport from the heated wall of the tube. It can be noted that similar trends are observed in all the experiments with other operating conditions. As vapor quality increase from 0.25 to 0.61, the heat transfer coefficient increases by about 63% for both R410A and R22.

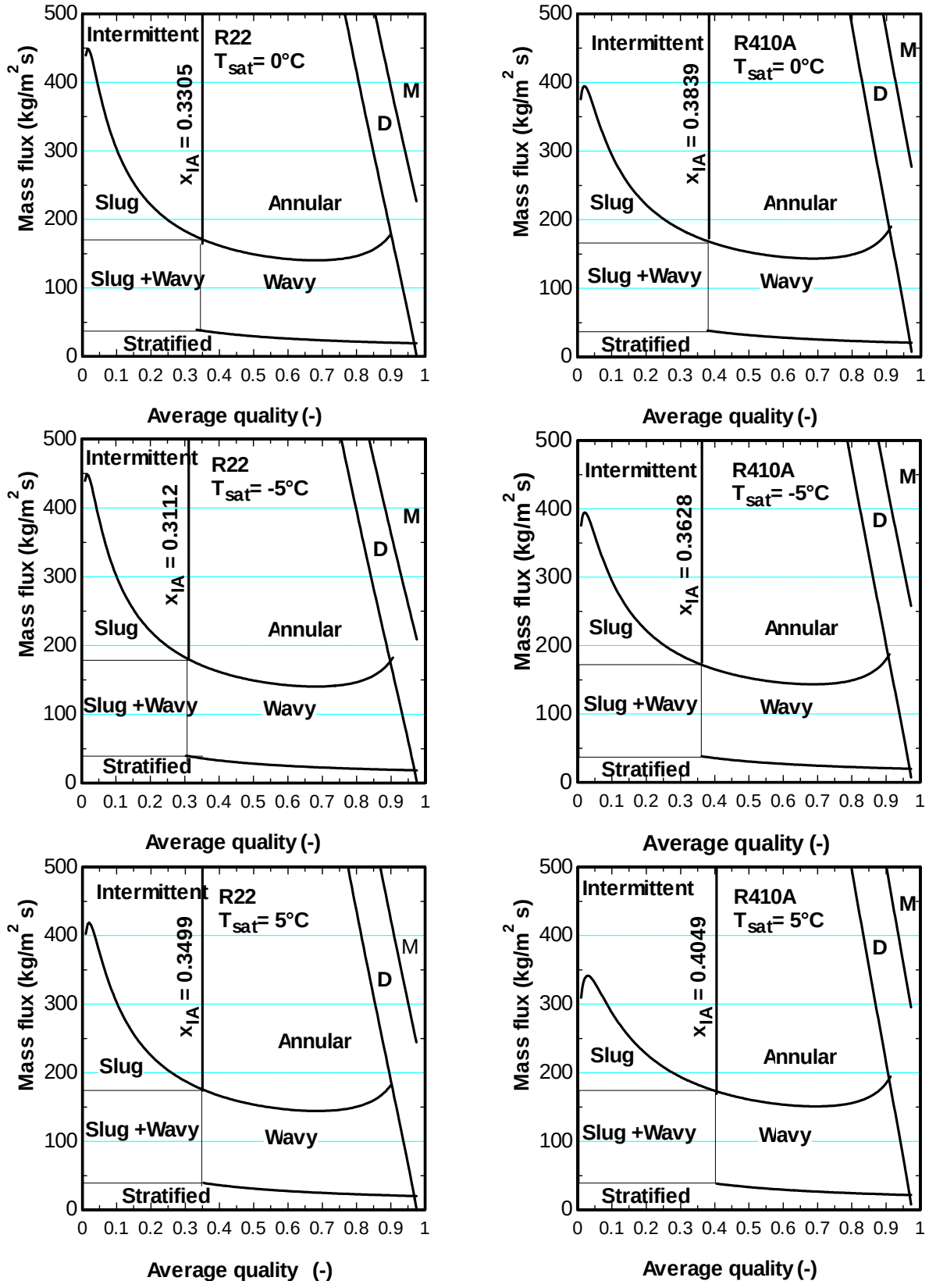

Figure 3. Flow pattern map at different operating conditions (**D** represents dryout zone and **M** represents mist flow)

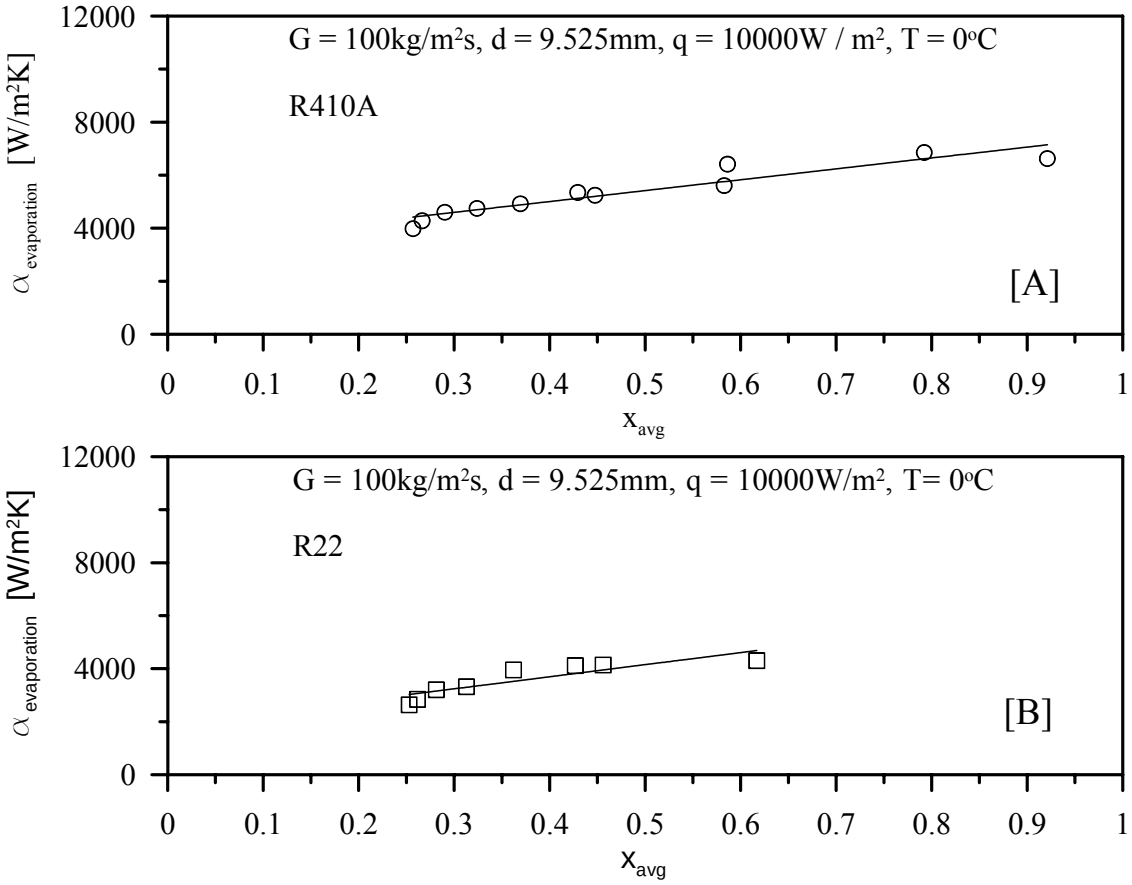

Figure 4. Heat transfer coefficients vs. vapor quality at different experimental conditions

4.2.2 Effect of heat flux on evaporative heat transfer

Flow pattern map for R410A and T_{sat} of 0ºC is shown in Figure 3. For G = 100 kg/s m^2 and vapor quality less than 0.38, it's clear that slug and stratified wavy flow occurs with moderate rise in heat transfer coefficient versus vapor quality; while, for G = 100 kg/s m^2 and vapor quality more than 0.38, stratified wavy occurs with increasing rise in heat transfer coefficient versus vapor quality. The heat transfer coefficients of R410A and R22 as a function of vapor quality at mass flux of 100 kg/m^2s and evaporating temperature of 0°C for heat fluxes are shown in Figure 5. It is clear that heat transfer coefficients of R410A and R22 increases with heat flux. For quality less than 0.58, heat transfer coefficients for R410A and R22 increases by about 31% and 51% at heat flux 10 kW/m^2 and increase by about 1% at high heat flux 29 kW/m^2, respectively. This can explained by fact that as heat flux increases, bubble departure frequency rapidly increases, and additional cavities of smaller sizes are activated on the heated surface. As a consequence, the nucleate boiling contribution increases. For quality more than 0.58 heat transfer coefficients for R410A increases by about 18% at heat flux 10 kW/m^2 and increases by about 15% at high heat flux 29 kW/m^2.

4.2.3 Effect of evaporating pressure on boiling heat transfer

The influence of the evaporating pressure on the heat transfer coefficient for R410A and R22 at a fixed refrigerant mass flux of 100 kg/m^2s, by varying the evaporating temperatures (-5 and 5ºC), at a heat flux of 10 kW/m^2 is shown in Figure 6 and Figure 7, respectively. It is clear that, heat transfer coefficients of R410A and R22 increase with evaporating pressure. In quality range 0.27:0.60, heat transfer coefficients for R410A increases by about 51% and 40% at T_{sat} of -5ºC and T_{sat} of 5ºC, respevtively. In quality range 0.20:0.42, heat transfer coefficients for R22 increases by about 56% and 32% at T_{sat} of -5ºC and T_{sat} of 5ºC, respectively. This can explained by fact that as ***pressure increases***, the contribution of ***nucleate boiling*** to the heat transfer coefficients ***increases***, mainly due to the corresponding decrease in the average bubble departure diameter for any given wall superheat. This effect induces the activation of additional new small cavities on the heated surface, thus increasing the number of active nucleation sites. Furthermore, under nucleate boiling, the product of bubble departure frequency and diameter is constant.

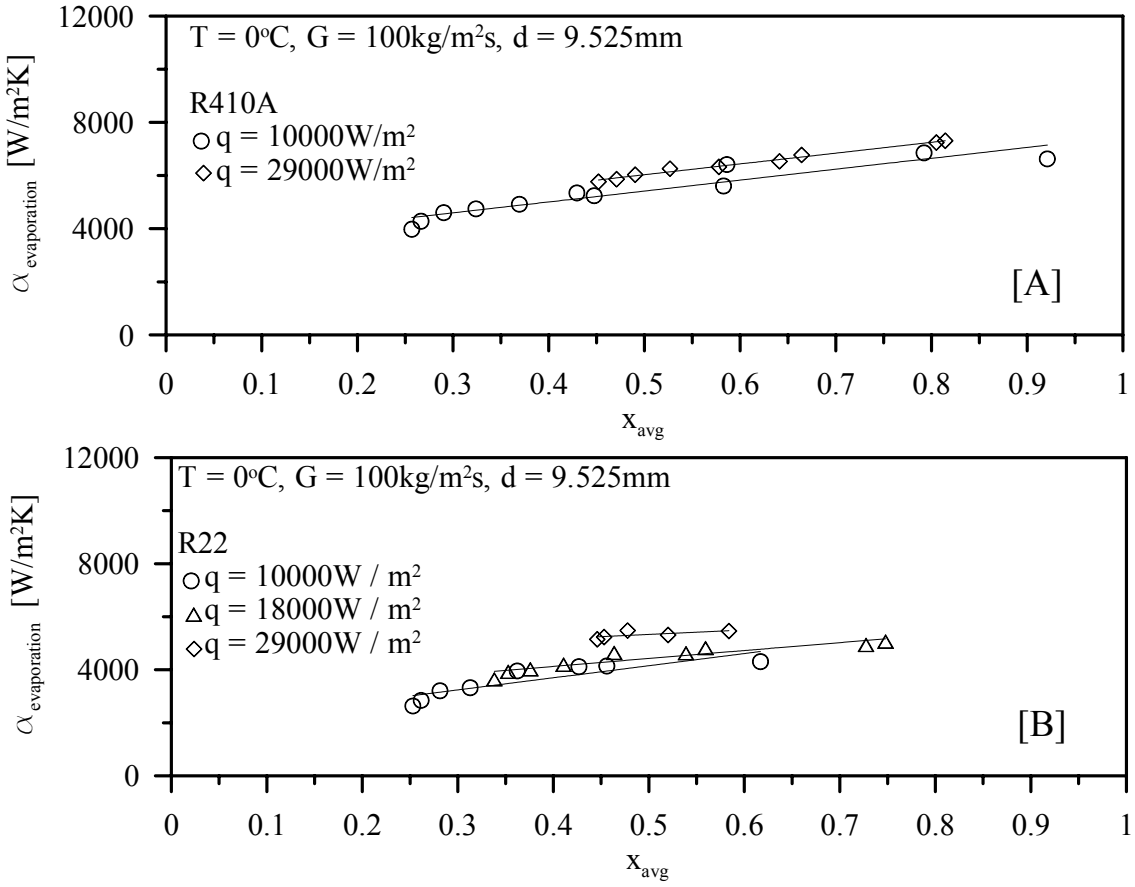

Figure 5. Heat transfer coefficients vs. vapor quality at different experimental conditions

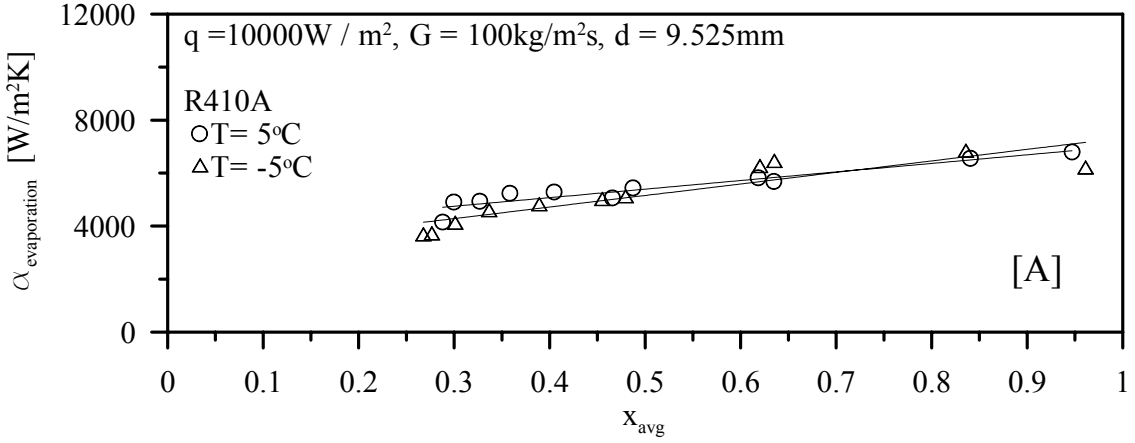

Figure 6. Heat transfer coefficients of R410A as a function of vapour quality varying evaporating temperature

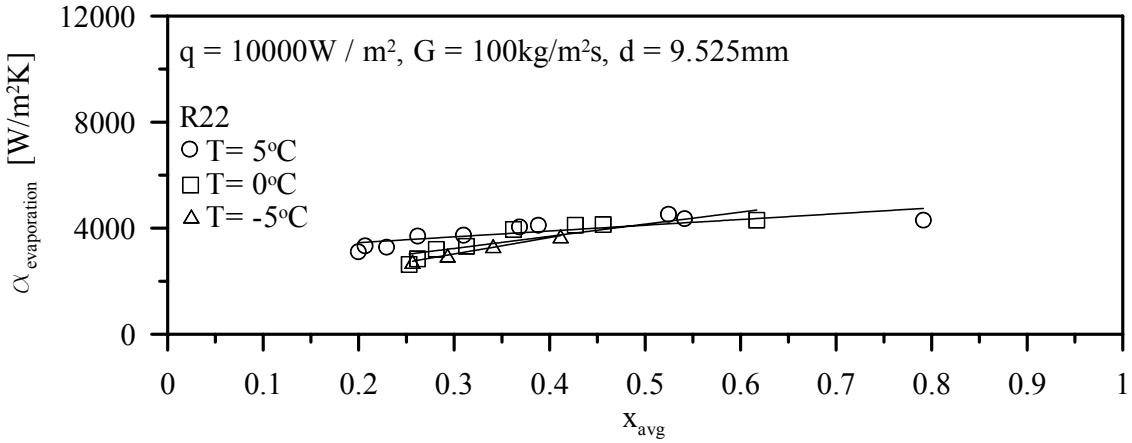

Figure 7. Heat transfer coefficients of R22 as a function of vapour quality varying evaporating temperature

At increased pressure, bubble frequency increases with decreasing bubble departure diameter, thus contributing to the increase of the heat transfer coefficient. For quality more than 0.60, heat transfer coefficient of R410A increase by about 16 % at both T_{sat} of -5ºC and T_{sat} of 5ºC. For quality more than 0.42, heat transfer coefficient of R22 increase by about 1 % at both T_{sat} of -5ºC and T_{sat} of 5ºC. This can explained by fact that the effect of pressure on convective boiling contribution mainly results from changes in fluid properties. This can explained by that, the vapor density increases with increasing pressure. Therefore, the higher average density of the vapor–liquid mixture leads a lower velocity at any given refrigerant mass flux. The liquid conductivity decreases, but the liquid specific heat increases and the liquid viscosity decreases. because the opposite effects tend to cancel one another lead to a weak effect of the pressure on convective contribution.

4.2.4 Comparison between R410A and R22 boiling heat transfer coefficients

The experimental data allow comparing the heat transfer coefficients of R410A and R22 at almost equal pressure, refrigerant mass-flux and heat flux. Figure 8 represents heat transfer coefficients of all the refrigerant fluids at a mass flux of 100 kg/m^{2}s, a heat flux of about 29 kW/m^2, and an evaporating temperature of about 5ºC. Table 2 summarizes the relevant thermo-physical properties of the refrigerants fluids in the operating conditions adopted in the experiments reported. It can be shown that, in the experiments corresponding to, R410A heat transfer coefficients are consistently better than those of R22, by a mean factor of about 14% and 17% at higher and lower values of evaporating pressures and heat fluxes, respectively. The heat transfer coefficient in ***convective boiling*** results from the ***interaction between nucleate boiling and liquid convection***. According to the Dittus–Boelter, single-phase forced convection correlation, the convective contribution to heat-transfer coefficient is directly proportional to the liquid property combination Ø:

$$\phi = \left(\frac{C_{PL}}{\mu_L} \right)^{0.4} \cdot k_L{}^{0.6} \tag{9}$$

Therefore, by increasing the value of Ø, the convective contribution to the heat transfer coefficient increases. The nucleate boiling contribution to the heat transfer coefficient is strongly affected by the heat flux, the vapor density, the superficial tension, the heat of vaporization. The greater **vapor density** of R410A, together with a lower **superficial tension** and a greater **enthalpy of vaporization**, leads to a greater contribution of **nucleate boiling**, as compared to that of R22. For higher evaporating pressures and heat fluxes,

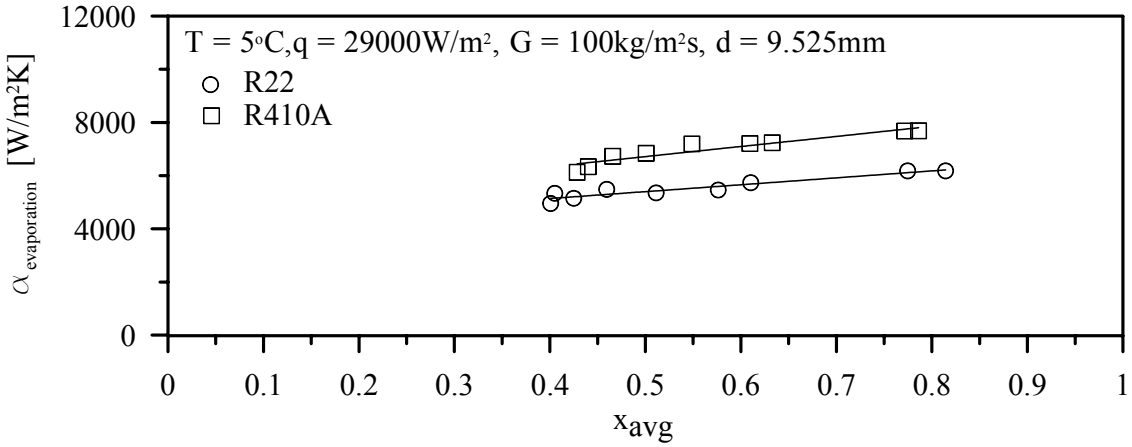

Figure 8. Heat transfer coefficients as a function of vapor quality varying the refrigerant fluid at G = 100 kg/m^{2}s, q = 29 kW/m^2, T_{sat} = 5ºC

Table 2. The thermo-physical properties affecting heat transfer

Fluid$	T_{sat} [C]	P_{sat} [bar]	ρ_G [kg/m3]	h_{fg} [J/kg]	C_{PL} [J/kg K]	k_L [W/m K]	μ_L [Pa s]	σ [N/m]	Ø Units*
R22	0	4.981	21.09	203843	1175	0.0946	0.0002043	0.012	122.9
R410A	0	7.985	30.64	222974	1524	0.1045	0.0001682	0.009	156.5
R22	5	5.843	24.62	199765	1189	0.0924	0.0001944	0.011	124.2
R410A	5	9.332	35.91	216539	1548	0.1013	0.0001574	0.009	158.7

* Ø units: $(J/kg\ K\ Pa\ s)^{0.4}(W/m\ K)^{0.6}$

i.e. for an increasing relative effect of nucleate boiling, the heat transfer coefficients of R410A become greater than that of R22, because of the greater nucleate boiling contribution (lower superficial tension, lower vapor density, greater enthalpy of vaporization) and greater Ø values of the latter.

4.2.5 Comparison of experimental results with existing correlations

The experimental results obtained with the test facility for R410A and R22 are presented in this section, together with the main findings.

The heat transfer results are compared with the Kattan model [16] and more conventional correlations such as Shah [20], Gungor [12], Bivens [9], Jung [14],…etc.

This comparison has been focused on the results from Kattan model [16] since it takes into account the flow regimes, and is based on the refrigerant physical changes occurring inside the tube.

The experimental results obtained for evaporation are compared with the correlations on parity plots in Figure 9.

These plots show the differences between experimental data and the calculated results obtained for the same test conditions. The figures show deviation between experimental and computed data for each correlation.

Points along the straight line show no difference between experimental and correlated data. Results above the 0% line are over-predicted by considered correlation and the ones below the 0% line are under-predicted. Dotted lines have been added to give an idea of the deviation between experimental and calculated values. This representation has been chosen to provide a visual and simple comparison of data. The main characteristics, determined from these parity graphs and the detailed results, are summarized below:

- The Shah [20] results under-predict the experimental data by a large amount deviation.

- The Biven correlation tends to under-predicted the experimental data by 30% deviation.
- The Gungor [12] correlation tends to under-predicted the experimental data by 30 to 40% deviation.
- The Jung [14] correlation tends to over-predicted the experimental data by 30% deviation and under-predicted by 30 to 50% deviation.
- The Hambraeus [13] tends to under-predicted the experimental data by 30% deviation.
- The Liu [18] correlation tends to over-predicted the experimental data by 30% deviation and under-predicted by 30% deviation, and kyu, Mathur [19], Kandlikar [15], Liven, Kuntha [17], Ohtatsuda [11] and Chaddock [10] correlations under-predict the experimental data by a large amount deviation.

It is worth noting that the difference between the correlations themselves is quite large and that they do not show a good agreement.

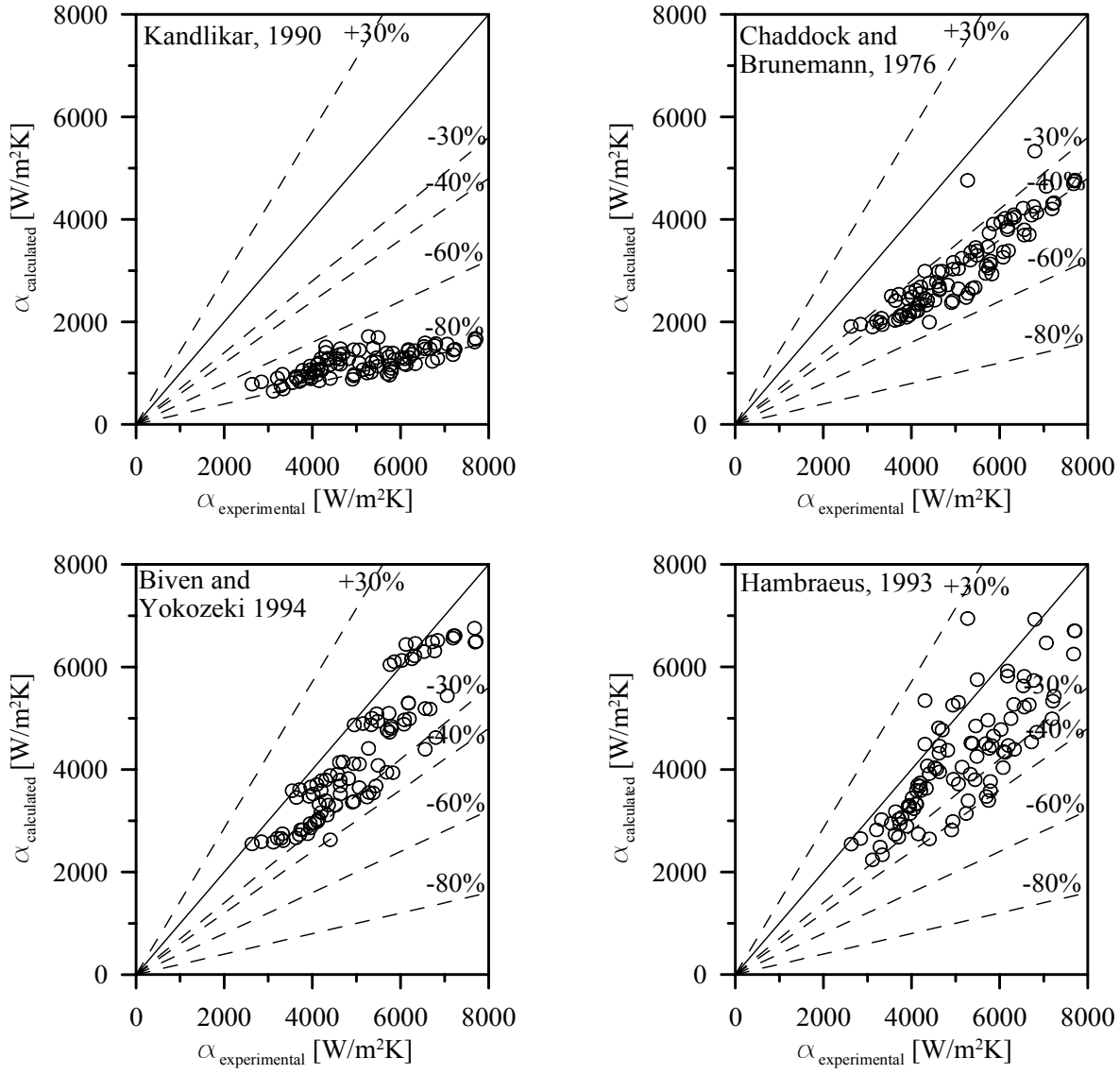

Figure 9. (a) Comparison of experimental data with the calculated correlations

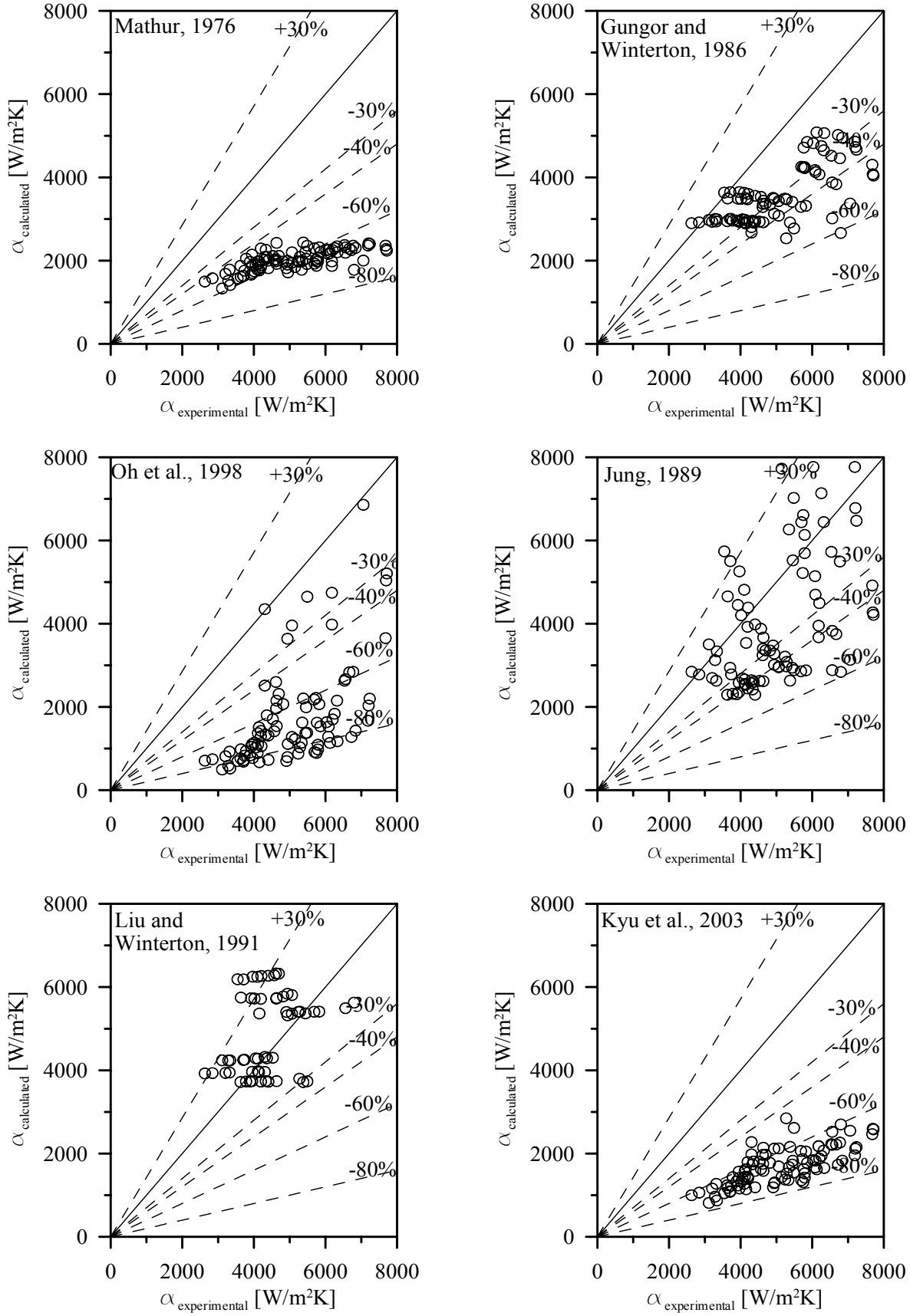

Figure 9. (b) Comparison of experimental data with the calculated correlations

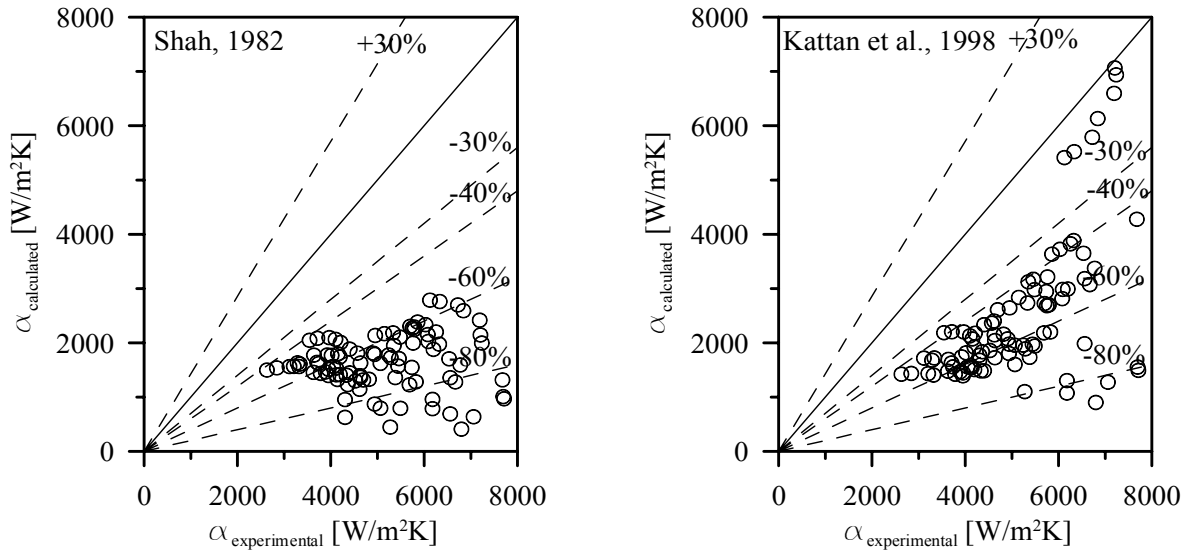

Figure 9. (c) Comparison of experimental data with the calculated correlations

4.2.6 Modification of Kattan correlation

A new correlation is proposed in this section based on the original Kattan model [16]. Modifications have been made to the original model to predict the local heat transfer coefficient results obtained with the test facility.

The Kattan model [16] characterized the convective boiling heat transfer coefficient with Equation (10), reproduced below:

$$\alpha_{cb} = C\,\mathrm{Re}_{\delta}^{m}\,\mathrm{Pr}_{L}^{0.4}\,\frac{k_L}{\delta} \tag{10}$$

This equation has two parameters, the leading constant C and the Reynolds number exponent m which have been redefined to fit the experimental results obtained in this study. The Kattan model [16] have been re-arranged in Equation (11) as suggested by Kattan et al. [16] to determine these two parameters for the present experimental results with R22 and R410A.

$$Y = \frac{\left[\dfrac{\left(2\pi\cdot\alpha_{\mathrm{exp.}} - \Theta_{dry}\cdot\alpha_g\right)^3}{\left(2\pi - \Theta_{dry}\right)^3} - \alpha_{nb}^3\right]^{1/3}}{\mathrm{Pr}_L^{0.4}\cdot\dfrac{k_L}{\delta}} = C\cdot\mathrm{Re}_{\delta}^{m} \tag{11}$$

By applying a logarithmic function to both sides of Equation(11), the equation becomes:

$$\ln Y = m\cdot\ln\mathrm{Re}_{\delta} + \ln C \tag{12}$$

Equation (12) is the equation of a straight line of slope m and intercept lnC which can be determined from the experimental data. Y and Re_{δ} have been calculated from the experimental results and their natural logarithm have been plotted in Figure 10.

The resulting coefficients for R410A and R22 have been determined from the equation of the straight line presented in Figure 10,

$$\ln Y = -2.50569 + 0.695658\cdot\mathrm{Re}_{\delta} \tag{13}$$

And the parameters were found as:

m = 0.695658

C = 0.081619

These coefficients C and m are to be used in conjunction with the Katttan model [16], and provide a correlation of the experimental data obtained in this study. The Kattan model [16] associated with these parameters is defined hereinafter as the "modified" Kattan model".The modified correlation was found to

be in much better agreement with the experimental results than the correlations from Gungor [12], Shah [20] and other correlations as shown in Figure 11.
This modified model is only valid for these experimental data with refrigerants R410A and R22 in the range defined below:
G = 100 kg/m^{2}s, q = 6 : 29 kW/ m^2 and T_{sat} = -5 : 5ºC, d = 9.525 mm.

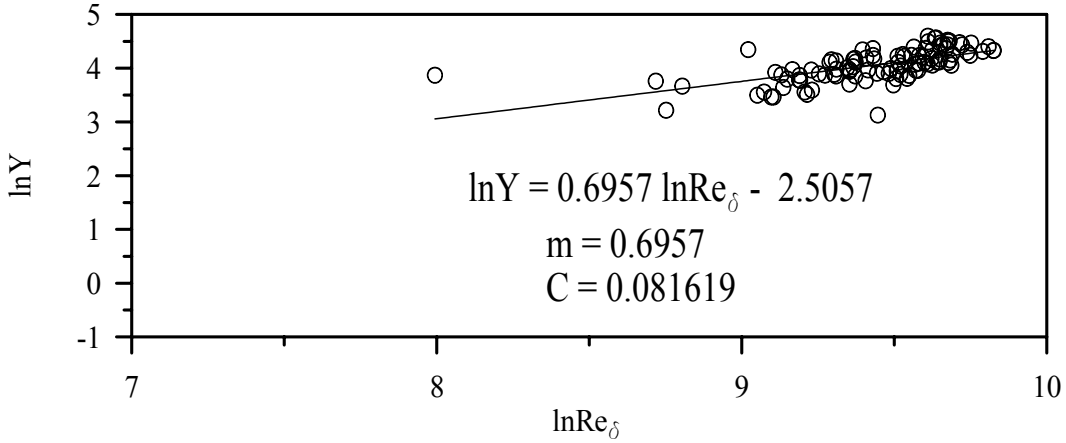

Figure 10. Determination of the parameters C and m, from the experimental results for R22 and R410A

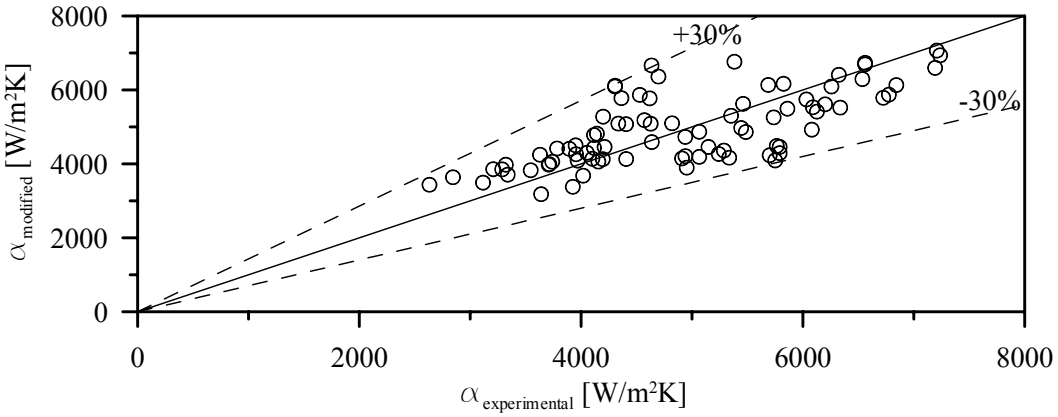

Figure 11. Comparison of experimental data with modified Kattan correlations

5. Conclusion

An experimental test rig is constructed for evaluating the heat transfer characteristics of pure and mixed refrigerants during convective boiling. The local heat transfer coefficients of R22 and R410A, are determined in a smooth horizontal tube during convective boiling.
In this work, the effects of the refrigerant vapor quality, saturation temperature, heat flux and thermo-physical properties on flow pattern maps and local heat transfer coefficient are analyzed in detail. From the experimental results, the following conclusions can be drawn:

- heat transfer coefficient of R410A and R22 increases with vapor quality. As quality increase from 0.25 to 0.61, heat transfer coefficient increases by about 63% for both R410A and R22.
- heat transfer coefficient of R410A and R22 depends upon the heat flux in the region of nucleate boiling between 0% and 50% vapor qualities. For quality more than 0.58, heat transfer coefficient for R410A increase by about 18% at heat flux 10 KW/m^2 and increase by about 15% at high heat flux 29 KW/m^2 .
- Heat transfer coefficients of R410A always increase with evaporating pressure. In quality range 0.27:0.60, heat transfer coefficient for R410A increase by about 51% and 40% at T_{sat} of -5ºC and T_{sat} of 5ºC, respectively. In quality range 0.20:0.42, heat transfer coefficient for R22 increase by about 56% and 32% at T_{sat} of -5ºC and T_{sat} of 5ºC, respectively. For quality more than 0.60, heat transfer coefficient of R410A increase by about 16 % at both T_{sat} of -5ºC and T_{sat} of 5ºC. For quality more than 0.42, heat transfer coefficient of R22 increase by about 1 % at both T_{sat} of -5ºC and T_{sat} of 5ºC.

- Heat transfer coefficients of R410A are better than those of R22, by about 17% and 14% at the lower and higher value of evaporating pressures and heat fluxes, respectively.

A new correlation is proposed in based on the original Kattan model [16]. Modifications have been made to the original model to predict the local heat transfer coefficient results obtained with the test facility.

Appendix

Fluid and Geometry Definition

Input D, x_{avg}, G, T_{sat}, q

Physical parameters from ESS. $\rho_L, \rho_G, \mu_L, \mu_g, \sigma, K_L, K_g$

Flow Pattern Boundaries Calculation

Stratified to Stratified Wavy transition is calculated from

$$G_{strat} = \left\{ \frac{(226.3)^2 A_{Ld} A_{Gd}^2 \rho_G (\rho_L - \rho_G) \mu_L g}{x^2 (1-x) \pi^3} \right\}^{1/3} \quad \text{(A1)}$$

Stratified Wavy to Intermittent /Annular boundary is calculated from the following equation

$$G_{wavy} = \left\{ \frac{16 A_{Gd}^3 g d_{in} \rho_L \rho_G}{x^2 \pi^2 \left(1-(2h_{Ld}-1)^2\right)^{0.5}} \left[\frac{\pi^2}{25 h_{Ld}^2} (1-x)^{-F_1(q)} \left(\frac{We}{Fr} \right)_L^{-F_2(q)} + 1 \right] \right\}^{0.5} + 50 \quad \text{(A2)}$$

Intermittent to Annular transition is calculated from the equation

$$x_{IA} = \left\{ \left[0.2914 \left(\frac{\rho_G}{\rho_L} \right)^{-1/1.75} \left(\frac{\mu_L}{\mu_G} \right)^{-1/7} \right] + 1 \right\}^{-1} \quad \text{(A3)}$$

Annular to Dryout boundary is calculated from

$$G_{dryout} = \left[\frac{1}{0.235} \left(\ln\left(\frac{0.58}{x} \right) + 0.52 \right) \left(\frac{d_{in}}{\rho_G \sigma} \right)^{-0.17} \cdot \left(\frac{1}{g d \rho_G (\rho_L - \rho_G)} \right)^{-0.37} \left(\frac{\rho_G}{\rho_L} \right)^{-0.25} \left(\frac{q}{q_{crit}} \right)^{-0.70} \right]^{0.926} \quad \text{(A4)}$$

Dryout to Mist is calculated from

$$G_{mist} = \left[\frac{1}{0.0058} \left(\ln\left(\frac{0.61}{x} \right) + 0.57 \right) \left(\frac{d_{in}}{\rho_G \sigma} \right)^{-0.38} \cdot \left(\frac{1}{g d \ \rho_G (\rho_L - \rho_G)} \right)^{-0.15} \left(\frac{\rho_G}{\rho_L} \right)^{0.09} \left(\frac{q}{q_{crit}} \right)^{-0.27} \right]^{0.943} \quad \text{(A5)}$$

Flow Pattern Classification

Stratified Flow Pattern	$G < G_{strat}$
stratified-wavy Flow Pattern	$G > G_{wavy}(x_{IA})$ gives the SLUG zone; $G_{strat} < G < G_{wav}(x_{IA})$ and $x < x_{IA}$ give the SLUG/STRATIFIED-WAVY zone; $x \geq x_{IA}$ gives the STRATIFIED-WAVY zone.
Intermittent Flow Pattern	$G_{wav} < G < G_{dryout}$ and $x < x_{IA}$
Annular Flow Pattern	$G_{wav} < G < G_{dryout}$ and $x > x_{IA}$
Dray out Flow Pattern	If $G_{strat} \geq G_{dryout}$, then $G_{dryout} = G_{strat}$ If $G_{wavy} \geq G_{dryout}$, then $G_{dryout} = G_{wavy}$
Mist Flow Pattern	If $G_{strat} \geq G_{mist}$, then $G_{mist} = G_{strat}$ If $G_{wavy} \geq G_{mist}$, then $G_{mist} = G_{wavy}$

Table A1. Flow pattern boundaries calculation for R410A,T=5

x_avg.	x_IA	G_mist	G_dryout	G_wavy	G_strat
0.01	0.4049			309.6	
0.109	0.4049			280.3	
0.208	0.4049			223.9	
0.307	0.4049			192.1	
0.406	0.4049			172.7	38.11
0.505	0.4049			160.4	32.9
0.604	0.4049			153.2	29.2
0.703	0.4049			150.9	26.43
0.802	0.4049		491	156	24.28
0.8253	0.4049		424.1	159.2	23.85
0.8544	0.4049		342.1	165.5	23.33
0.8835	0.4049		261.2	175.6	22.85
0.9126	0.4049	467.7	181	193.6	22.39
0.9418	0.4049	384.3	100.3	230.3	21.96
0.9709	0.4049	302.4	15.9	338.2	21.56

Nomenclature

D	Diameter (m)
G	Mass flux (kg/m^2 s)
α	Heat transfer coefficient (W/m^{2}K)
I	Current (A)
h	Specific enthalpy (J/kg)
k	Thermal conductivity (W/m K)
$\dot{m}$	Mass flow rate (Kg/s)
P	Pressure (Pa)
q	Heat flux (W/m^2)
Q	Heat transfer rate (W)
T	Temperature (K)
V	Voltage (volt)
x	Vapor quality (---)
ΔP	Pressure drop (Pa)
ΔT	Temperature difference (K)
Δx	Change in quality (---)

Greek letters

Δ	Differential (---)
μ	Dynamic viscosity (Pa.s)
ν	Kinematics viscosity (m^2/s)

Subscripts

G	gas
L	liquid
o	outside
r	Refrigerant
sat	Saturation
tp	two-phase

References

[1] ASHRAE, 1997, "ASHRAE Handbook-Fundamentals", American Society of Heating, Refrigerating and Air conditioning Engineers, Atlanta, Georgia, USA.

[2] Kim, Y., Seo, K., and Chung, J.T., 2002, "Evaporation heat transfer characteristics of R410A in 7 and 9.52 mm smooth/micro-fin tubes", I.J. of Refrig., vol. 25, pp. 716-730.

[3] Kyu, O.H., Taek, O.J., Chun, J.J., and Woo,H.J., 2003, "Study on the evaporating flow patterns and heat transfers of R22 and R134a in small diameter tubes" International congress of Refrigeration, Washington, D.C., pp. 1-7.

[4] Greco, A., 2007, "Convective boiling of pure and mixed refrigerants: An experimental study of the major parameters affecting heat transfer", I.J. Heat and Mass Transfer, Vol. 15, pp. 896-909.

[5] Shin, J.Y., Kim, M.S., and Ro, S.T., 1997, "Experimental study on forced convection boiling heat transfer of pure refrigerants and refrigerant mixtures in a horizontal tube", I. J. Refrig., Vol. 20, No. 4, pp. 2677-275.

[6] Zhang, X., and Yuan, X., 2008, "Heat transfer correlations for evaporation of refrigerant mixtures flowing inside horizontal microfin tubes", Energy Conversion and Management, Vol. 49, pp. 3198-3204.

[7] Mcjimsey, B.A., 1994,"Experimental investigation of the effect of oil on convective heat transfer and pressure drop of R410A inside smooth tube", doctoral Thesis, Texas A&M university, pp. 22-138.
[8] Park, C.Y. and Hrnjak, P.S., 2007, "CO2 and R410A flow boiling heat transfer, pressure drop, and flow pattern at low temperatures in a horizontal smooth tube", Int. J. Refrig., vol. 30, pp. 166-178.
[9] Bivens, D.B. and Yokozeki, A., 1994,"A Heat transfer of zeotropic refrigerant mixtures heat pumps for energy efficiency and environmental progress", Elsevier, Amsterdam.
[10] Chaddock, J.B. and Brunemann, H. 1967, "Forced convection boiling of refrigerants in horizontal tubes", Report HL-113, Duke University,Durham.
[11] Oh, Hoo-Kyu, Katsuta, M. and Shibata, K, 1998,"Heat transfer characteristics of R134a in a capillary tube heat exchanger", Proceedings of 11th IHTC. Vol. 6, pp. 131-136.
[12] Gungor, K. E., and Winterton R.H.S., 1986, "A general correlation for flow boiling in tubes and annuli", I.J. Heat Mass Transfer, Vol. 29, No. 3.
[13] Hambraeus, k., 1993, "Flow boiling of pure and oil contaminated refrigerants: heat transfer and pressure drop in a horizontal tube", doctoral Thesis, Personal Communication.
[14] Jung, D. S., May 1989, "Horizontal- Flow boiling heat transfer using refrigerant mixtures", EPRIER 6364, Project 8006-2, Final Report.
[15] Kandlikar, S.G., 1990, "A general correlation for saturated two-phase flow boiling heat ransfer inside horizontal and vertical tubes", J. of Heat Transfer, Vol. 112, Feb., pp. 219-228.
[16] Kattan, N., Thome, J. R., and Favrat, D., 1998, "Flow boiling in horizontal tubes: Part 2 - new heat transfer data for five refrigerants", J. Heat Transfer. Vol. 120, pp. 148–155.
[17] Kuntha, U. and Kiatsiriroat, T., 2002,"Boiling heat transfer coefficient of R-22 refrigerant and its alternatives in horizontal tube : small refrigerator scale", Songklanakarin J. Sci. Technol., Vol. 24, No. 2, pp. 243-253.
[18] Liu, Z., and Winteron, R.H.S., 1991, "A general correlation for saturated and subcooled flow boiling in tubes and annuli, based on nucleate pool boiling Equation", I. J. Heat Mass Transfer, Vol. 34, No. 11, pp. 2759-2766.
[19] Mathur, A.P., 1976, "Heat transfer to oil-refrigerant mixtures evaporating in tubes", PhD thesis, Duke Univ.
[20] Shah, M. M., 1982, "Chart correlation for saturated boiling heat transfer: equations and further study", ASHRAE Trans., Vol. 88, Part 1, pp.185-196.
[21] Wojtan, L., Ursenbacher, T., and Thome, J. R. 2005, "Investigation of flow boiling in horizontal tubes: Part I - A new diabatic two-phase flow pattern map", I. J. Heat Mass Transfer, Vol. 48. pp. 2955–2969.

M. Fatouh is prof. lecturer in Mechanical Power Engineering Department, Faculty of Eng., Helwan Uni., Cairo, Egypt. He has obtained his Ph.D. from Indian Institute of Technology Madras. His major research area is Refrigeration and Air-conditioning. He has about 19 years of teaching and research experience.
E-mail address: drmohfat@hotmail.com, Tel.: +2 -010 625 2404

A.B.Helali is Assist prof. lecturer in Mechanical Power Engineering Department, Faculty of Eng., Helwan Uni., Cairo, Egypt. He has obtained his Ph.D. from the same univ. His major research area is Heat and Mass Transfer Applications. He has about 19 years of teaching and research experience.

M.A.M. Hassan is doctor lecturer in Mechanical Power Engineering Department, Faculty of Eng., Helwan Uni., Cairo, Egypt. He has obtained his Ph.D. from Denmark Technical Univ. His major research area is Heat and Mass Transfer Applications. He has about 12 years of teaching and research experience.

A. Abdala is teach Ass. lecturer in Mechanical Power Engineering Department, Faculty of Eng., Helwan Uni., Cairo, Egypt. He has obtained his M.Sc.. from the same Univ. in years 2010. His major research area is Heat and Mass Transfer Applications. He has about 6 years of teaching and research experience.
E-mail address: antar451@yahoo.com, Tel.: 0086 -15134554005.

